HYDROLOGICAL PROCESSES
Hydrol. Process. (2010)
Published online in Wiley InterScience
(www.interscience.wiley.com) DOI: 10.1002/hyp.7601

Runoff–infiltration partitioning using an upscaled Green–Ampt solution

J. R. Craig,* G. Liu and E. D. Soulis
Department of Civil and Environmental Engineering, University of Waterloo, Waterloo, ON, Canada N2L 3G1

Abstract:

A new set of formulae for calculating regionally averaged infiltration rates into heterogeneous soils is presented. The solutions are based upon an upscaled approximation of the explicit Green-Ampt (GA) infiltration solution, and require specification of the spatial distribution of saturated hydraulic conductivity and/or initial soil water deficit in the sub-basin. The resultant areal averaged infiltration formulae, which ignore the impacts of run on or spatial correlation, are easily integrated into existing distributed surface water schemes, and can also be used to calculate saturated soil surface area. The impacts of preferential flow may be investigated through the use of a bimodal conductivity distribution. The solutions are tested against Monte Carlo simulations and assessed for accuracy. Interesting results are obtained regarding the impacts of upscaling on GA infiltration, most notably that the cumulative infiltration is most impacted by low-conductivity soils and that calibration of the standard (point-scale) GA equation to basin-scale hydrographs will lead to an underestimation of average system hydraulic conductivity. Copyright © 2010 John Wiley & Sons, Ltd.

KEY WORDS Green-Ampt; upscaling; soil heterogeneity; infiltration

Received 28 August 2009; Accepted 7 December 2009

INTRODUCTION

The determination of infiltration rates into saturated and unsaturated soils is of critical importance in hydrological modelling. The quantity of infiltration determines the amount of water available for runoff, evaporation, root uptake, and recharge to the groundwater beneath. In detailed physically based models (e.g. SHE (Abbott *et al.*, 1986)), heterogeneous infiltration processes may be simulated to a high degree of precision by numerically solving Richards equation, which governs flow in saturated and unsaturated porous media. However, for regional-scale lumped models and land surface schemes, computational expediency and lack of detailed soil data demands that researchers use a more approximate parameterization of the runoff–infiltration partitioning relationship. Many existing models (e.g. CLASS (Verseghy, 1991), WEPP (Flanagan and Nearing, 1995), HSPF (Bicknell *et al.*, 2001), or SWAT (Neitsch *et al.*, 2002)) use the Green–Ampt (GA) equation (Green and Ampt, 1911) for these purposes. Because the GA infiltration equation is an analytical solution to Richards equation, the physical meaning of model parameters ostensibly correspond to soil properties that are measurable in the field. A critical drawback of this approach is that it does not explicitly account for the inevitable heterogeneity at the sub-basin (or computational) scale, which has been shown to have a significant impact upon the response of a watershed soils to a rainfall event (Sharma *et al.*, 1980; DeRoo *et al.*, 1992).

Recognizing that heterogeneity of saturated hydraulic conductivity is a significant driver of net basin infiltration, researchers have attempted to develop general upscaled expressions for infiltration based upon direct upscaling of point-scale governing equations (Chen *et al.*, 1994) or of point-scale infiltration solutions (Maller and Sharma, 1981; Dagan and Bresler, 1983; Sivapalan and Wood, 1986; Smith and Goodrich, 2000; Govindaraju *et al.*, 2001). These expressions were of varying complexity, with later extensions addressing complex lateral relationships such as run on (Corradini *et al.*, 2002), spatial correlation (Govindaraju *et al.*, 2001), and rainfall variation (Morbidelli *et al.*, 2006). While all are theoretically sound within the bounds of their assumptions, these solutions individually suffer from an inability to closely match computational (i.e. Monte Carlo) solutions for the complete range of soil textures, as demonstrated by Corradini *et al.*, (2002). This, in part, is due to lower-order approximations used for the GA equation at the point scale (e.g. that of (Philip, 1957)) or empirical approximations that have not been tested under the full range of parameters (Smith and Goodrich, 2000; Govindaraju *et al.*, 2001). Most of the approaches additionally require some form of series expansion, Monte Carlo simulation, numerical integration, or Latin Hypercube sampling in order to generate the expected value of infiltration rates (Dagan and Bresler, 1983; Govindaraju *et al.*, 2001; Corradini *et al.*, 2002), and may perhaps be considered too complex to include in many land surface schemes.

* Correspondence to: J. R. Craig, Department of Civil and Environmental Engineering, University of Waterloo, Waterloo, ON, Canada N2L 3G1. E-mail: jrcraig@uwaterloo.ca

Here, an alternative direct method for upscaling the GA solution for laterally heterogeneous soils is presented. It is based upon a new and accurate approximation of the explicit GA formulation. The method addresses not only spatial variability in hydraulic conductivity (as addressed by Maller and Sharma (1981); Dagan and Bresler (1983); Sivapalan and Wood (1986); Govindaraju *et al.*, (2001); Corradini *et al.*, (2002)) but also variability in initial saturation, porosity, and/or wetting front matric potential. Results are compared to Monte Carlo simulations of spatially random infiltration without run on.

THE GA INFILTRATION MODEL

The point infiltration equation developed by Green and Ampt (1911) extended to conditions of non-immediate ponding Mein and Larson. (1973); Chow *et al.* (1988) is typically presented in terms of cumulative infiltration, $F(t)$, as a function of time, t (e.g. Dingman (2002)):

$$F(t) = \begin{cases} wt & \text{for } t \le t_p \\ F(t_p) + \alpha \ln\left(\dfrac{F(t)+\alpha}{F(t_p)+\alpha}\right) & \\ \quad + k_s(t - t_p) & \text{for } t > t_p \end{cases} \tag{1}$$

where w is the constant rainfall rate, $\alpha = |\psi_f|(\theta_s - \theta_0)$, ψ_f is the wetting front suction head, θ_0 is the (uniform) initial moisture content, θ_s is the soil porosity, k_s is the saturated hydraulic conductivity of the soil, and t_p, the time to ponding, is given by:

$$t_p = \frac{\alpha k_s}{w(w - k_s)} \tag{2}$$

Given the cumulative infiltration, $F(t)$, the infiltration rate, $I(t) = dF/dt$ may be calculated as:

$$I(t) = \begin{cases} w & \text{for } t \le t_p \\ k_s\left(1 + \dfrac{\alpha}{F(t)}\right) & \text{for } t > t_p \end{cases} \tag{3}$$

While most discussions of the GA formulation focus on the evolution of infiltration rate over time, it is revealing to plot infiltration rate as a function of k_s, as shown in Figure 1. Here, the dimensionless time parameter, X, varies from $X = 0$ at $t = 0$ to $X = 1$ at $t = \infty$, and is defined as follows:

$$X = \frac{1}{1 + 1/(w/\alpha)t} \tag{4}$$

The curves in this figure are snapshots in time: for a given conductivity, the infiltration rate decreases with increasing X from $I(0) = w$ with $X = 0$ to $I(\infty) = k_s$ with $X = 1$, as expected. The objectives of this paper are to first identify appropriate (integrable) approximations for these curves, then to use these in order to develop simple explicit expressions for areal-averaged infiltration

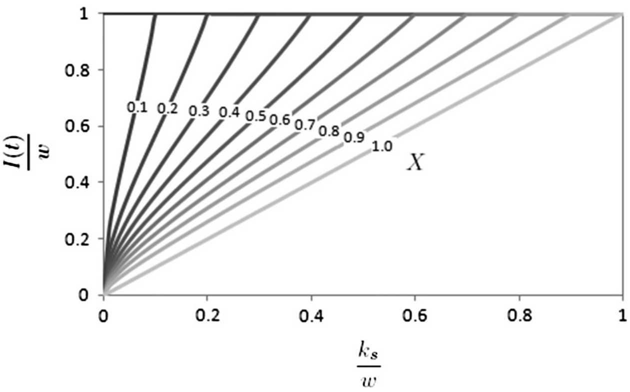

Figure 1. Dimensionless Green-Ampt infiltration rate as a function of dimensionless conductivity. Individual curves correspond to snapshots of dimensionless time, X, which progresses from $X = 0$ at $t = 0$ to $X = 1$ at $t = \infty$. For the definition of X, see text

rate subject to a known distribution of saturated conductivity and/or α.

Once a reasonable approximation for infiltration rate as a function of conductivity is found, the mean infiltration rate for heterogeneous media and/or heterogeneous initial conditions may be obtained by application of simple statistical laws. For the case of homogeneous initial conditions and heterogeneous conductivity, the mean infiltration rate, $\bar{I}$, may be calculated as:

$$\bar{I}(t) = \int_0^\infty I(X(t), k_s) \cdot f_k(k_s) dk_s \tag{5}$$

where f_k is the probability distribution function (pdf) of saturated hydraulic conductivity within the modelled domain. Conductivity is here assumed to be a random variable represented using a standard log–normal distribution:

$$f_k(k_s) = \frac{1}{k_s \sigma_Y \sqrt{2\pi}} \exp\left(-\frac{(\ln(k_s) - \mu_Y)^2}{2\sigma_Y^2}\right) \tag{6}$$

where μ_Y and σ_Y are the mean and standard deviation of log hydraulic conductivity. A more general expression is available for the case of general variability in both conductivity, initial moisture deficit, and/or wetting front matric potential:

$$\bar{I}(t) = \int_0^\infty \int_0^\infty I(X(t, \alpha), k_s) \cdot f_{k\alpha}(k_s, \alpha) d\alpha dk_s \tag{7}$$

where $f_{k\alpha}$ is the joint probability distribution of saturated conductivity and α. It is assumed here that there is no lateral relationship between vertical soil columns, either statistically (in the form of spatial correlation) or physically (in the form of run on processes). The implications of these assumptions are addressed elsewhere (Corradini *et al.*, 2002; Govindaraju *et al.*, 2001).

APPROXIMATIONS TO THE I-K_S CURVES

While usually expressed in implicit form (as in Equation 1), the GA solution may be formulated explicitly. Here,

DOI: 10.1002/hyp

the authors have identified alternative approximations to Equation 3 that are more amenable than those previously proposed (e.g. Barry *et al*., (2005)) to closed-form integration with respect to both k_s and α. It is clear from Figure 1 that a reasonable first approximation of infiltration rate may be given by the linear approximation:

$$I(t) = \min\left(w, \frac{k_s}{X}\right) + \varepsilon(X, k_s) \quad (8)$$

where $\varepsilon(X, k_s)$ is the deviation of the exact solution from the linear approximation, plotted in Figure 2. The linear approximation of Equation 8 is exact at the endpoints ($k_s/w = 0$ and $k_s/w \geq X$), and diminishes in quality for reduced ratios of conductivity to rainfall rate. As apparent in Figure 2, an error of up to ~13·5% is possible for small conductivities at early times. Equation 8 will be used as the starting point for the approximation used here, and an attempt is made to identify a viable (and integrable) approximation to $\varepsilon(X, k_s)$.

Upon substitution of Equations 6 and 8 into Equation 5, the first-order contribution to the mean infiltration rate may be directly evaluated using basic calculus, leading to the following first approximation for average infiltration:

$$\bar{I}(t) = \frac{w}{2}\mathrm{erfc}\left(\frac{\ln(wX) - \mu_Y}{\sigma_Y\sqrt{2}}\right) + \frac{w}{2wX}\exp\left(\mu_Y + \frac{\sigma_Y^2}{2}\right) \mathrm{erfc}\left(\frac{\sigma_Y}{\sqrt{2}} - \frac{\ln(wX) - \mu_Y}{\sigma_Y\sqrt{2}}\right) + w\int_0^{X(t)} \varepsilon(X(t), k_s) \cdot f_k(k_s)\mathrm{d}k_s \quad (9)$$

Where the remaining epsilon term still must be evaluated numerically. The ε function was here approximated using curve fitting techniques. The 'true' surface used for fitting was generated using the iterative approximation of (Barry *et al*., 2005). The best approximation found was given by:

$$\varepsilon \approx 0{\cdot}3632 \cdot (1 - X)^{0{\cdot}484} \cdot \left(1 - \frac{k_s}{wX}\right)^{1{\cdot}74} \left(\frac{k_s}{wX}\right)^{0{\cdot}38} \quad (10)$$

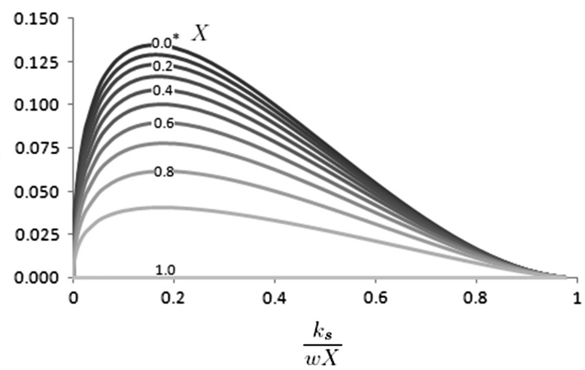

Figure 2. Dimensionless error in the linear approximation, ε, as a function of dimensionless conductivity, normalized to the dimensionless time parameter, X. The curve labelled 0·0* is the limit of ε as X approaches zero

resulting in a maximum error of 0·006 w (0·6% error), acceptable for nearly all modelling applications, especially considering the errors from ignoring heterogeneity are significantly larger. With this approximation, the remaining integral in Equation 9 can be evaluated quite effectively with simple single-interval two-point Gauss quadrature.

Figure 3 depicts the difference in behaviour between the standard GA model and the upscaled version used here for a number of different mean dimensionless conductivities with the same coefficient of variation. Notably, the upscaling process smooths out the threshold behaviour of the basin, as the ponding time is no longer a fixed point in time. Rather, different locations in space reach saturation at different points in time. Regardless of the degree of heterogeneity, the cumulative infiltration (which is linked with the total volume under the curve) is less than that predicted with the point-scale solution.

The approach above is not strictly limited to a simple log–normal distribution. A simple and useful revision is to represent the influence of preferential flow via the use of a bimodal log–normal distribution, where the conductivity distribution function is written as the sum of two log–normal distributions, i.e. $f_k(k_s) = (\omega)f_1(k_s) + (1 - \omega)f_2(k_s)$, where ω is a weight coefficient ($0 < \omega < 1$) and f_1 and f_2 have unique means and standard deviations. Because integration is a linear operator, the average solution is easily obtained through the application of Equation 9 for each component.

An interesting by-product of the formulation derived above is that the evolution of saturated area, A_s, during a storm event may be determined as the total area of the basin, A, multiplied by the percentage of saturated ground at any point in time:

$$A_s(t) = A\int_0^{(\frac{w}{k_s}-1)wt} \int_0^{wX} f_{k\alpha}(\alpha, K)\mathrm{d}k_s \mathrm{d}\alpha \quad (11)$$

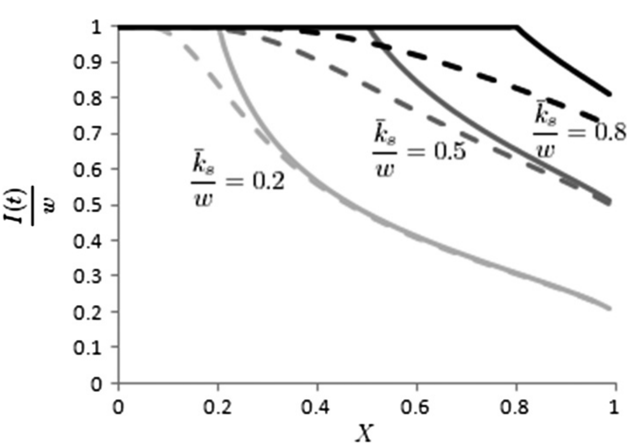

Figure 3. Evolution of dimensionless infiltration rate with the dimensionless time parameter for standard (solid) and upscaled (dashed) GA solutions. Three different ratios (0·2,0·5,0·8) of average conductivity to rainfall rate are depicted. The coefficient of variation ($\bar{k}_s/\sigma_k$) for all three upscaled models was kept fixed at 0·5

DOI: 10.1002/hyp

Which for a log–normal k_s distribution and fixed α leads to

$$A_s(t) = A\int_0^{wX} f_k(k_s)\mathrm{d}k_s = \frac{A}{2}\left[1 - \mathrm{erf}\left(\frac{\mu_Y - \ln(wX)}{\sqrt{2}\sigma_Y}\right)\right] \quad (12)$$

where, combining Equations 2 and 4, wX is the maximum value of k_s producing saturation at time t.

Figure 4 illustrates the differences in the transient evolution of surface saturation for varying degrees of heterogeneity in k_s. Here, $\overline{k}_s = 0{\cdot}4\ w$. Instead of the abrupt switch from unsaturated to saturated surface predicted by the classic GA model, the upscaled version appropriately depicts a gradual transition, with some of the soil surface saturating well before the mean ponding time, and some (the soil with a hydraulic conductivity greater than the rainfall rate) staying perpetually dry. The evolution of this process spreads out as heterogeneity increases.

VARIABLE INITIAL SOIL MOISTURE/WETTING FRONT SUCTION

Unlike conductivity, which is known to be well-represented using a log–normal distribution, spatial variation of the aggregate parameter $\alpha = \psi_f|\theta_s - \theta_0|$ is not well-characterized in the literature. The wetting front matric potential, ψ_f, is a function of soil texture and the form of the characteristic soil curves (Neuman, 1976), and is therefore correlated to conductivity. It varies roughly linearly with log conductivity, ranging from about 10 cm for sands up to 100 cm for clays, and can be reasonably well-characterized with a normal distribution. Presumably, the initial saturation deficit, $S_d = |\theta_s - \theta_0|$ can also be represented using a normal distribution (Patgiri and Baruah, 1995), but due to the presence of fixed upper and lower bounds is likely better represented using a beta or uniform distribution (Haskett *et al.*, 1995; Det Norske Veritas, 1997). Multiple field studies of soil moisture distributions have discovered wildly varying distributional characteristics, depending upon characteristics as varied as soil texture, storm duration, vegetation, soil organic content, and season (Sharma *et al.*, 1980; Merzougui and Gifford, 1987; Miller *et al.*, 2007; Famiglietti *et al.*, 2008; Lakhankar *et al.*, 2009). Due to the large variation in infiltration behaviour from site to site, and the significant number of unknown correlations between variables, it is likely impossible in this case to choose one 'correct' distribution of α. Instead, we will assume here for the purpose of mathematical simplicity that α is appropriately represented with a normal distribution characterized by a mean μ_α and standard deviation σ_α. To avoid non-negativity, it is recognized that the negative portion of the distribution corresponds to a finite probability of α being equal to zero (i.e. the area under the negative portion of the normal distribution corresponds to the percentage of soil initially saturated). It is assumed that these distribution parameters may be either calibrated or estimated from known or approximated distributions of ψ_f, θ_i, and θ_s. Under these conditions, the function $1/X$ also satisfies a normal distribution, and we are able to once again obtain a simple formula for $\overline{I}(t)$ subject to a distribution of soil properties, in this case, variability in initial moisture content and/or wetting front potential subject to a fixed hydraulic conductivity:

$$\begin{aligned}\overline{I}(t) = {} & \frac{w}{2} + \frac{w}{2}\mathrm{erfc}(A) + k_s\mathrm{erfc}(B) \\ & + k_s\left(1 + \frac{\mu_\alpha}{wt}\right)\frac{1}{2}[\mathrm{erfc}(A) - \mathrm{erfc}(B)] \\ & + \frac{k_s}{wt}\frac{\sigma_\alpha}{\sqrt{2\pi}}[\exp(-B^2) - \exp(-A^2)] \\ & + w\int_0^{(\frac{w}{k_s}-1)wt} \varepsilon(X(\alpha, t), k_s) f_\alpha(\alpha)\mathrm{d}\alpha \quad (13)\end{aligned}$$

where $A = (\mu_\alpha - (w/k_s - 1)wt)/(\sqrt{2}\sigma_\alpha)$ and $B = \mu_\alpha/(\sqrt{2}\sigma_\alpha)$. Once again, the limit of this expression as $\sigma_\alpha \to 0$ is the original expression from Equation 8.

Both solutions (Equations 9 and 13) are unique when compared to previous solutions proffered in the literature. Firstly, they are valid over the entire range of parameters and times. They correctly converge upon the standard GA equation in the limit as σ_Y and σ_α go to zero, a feat unattainable by the empirical approximations of Smith and Goodrich (2000). Lastly, because the solutions are cast in terms of the chosen dimensionless quantities, numerical integration of the ε integral is not sensitive to the particular set of parameters; any scheme that works appropriately in dimensionless space is appropriate for all possible model configurations. This, along with the relative simplicity of the solution, encourages inclusion in existing hydrological models.

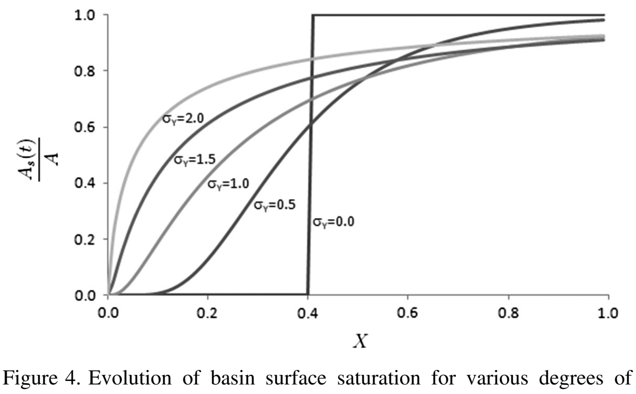

Figure 4. Evolution of basin surface saturation for various degrees of heterogeneity in hydraulic conductivity. X is the dimensionless time parameter

TESTING

To test the validity of the above derivations and demonstrate some of the interesting products of this approach, the solution has been directly compared to results of a Monte Carlo model. For the first test case, a heterogeneous domain was generated using 25 000 parcels with conductivities that satisfy the log–normal pdf with standard deviations of $\sigma_Y = 0{\cdot}1$, 0·5, 1·0, and 2·0, and mean dimensionless conductivity of $\overline{k}_s/w = 0{\cdot}4$ ($\overline{k}_s =$ 1·6 cm/h). This was repeated for a dimensionless conductivity of $\overline{k}_s/w = 0{\cdot}1$, to survey the range of possible responses. Since only vertical processes are considered here, spatial correlation is ignored. For the Monte Carlo simulation, the value of α was specified as 3 cm; however, the curves are valid for all soils with this conductivity/rainfall ratio, as the dimensionless time parameter, X fully encapsulates the impacts of variation in α. The average and cumulative infiltration into the heterogeneous soil were calculated using both the Monte Carlo approach and Equation 9. Results are depicted in Figure 5a and b. It is clear that for both cases, the semi-analytical upscaling is a very good approximant to the Monte Carlo simulations: maximum errors are on the order of 3%, and are entirely due to the approximation of the ε integral in Equation 9, which was evaluated using single interval two-point Gauss–Legendre quadrature. For all practical purposes, the analytical and Monte Carlo solutions may be considered identical in output. Similar results are obtained for other values of $\overline{k}_s/w$.

An identical test was run for the variable initial saturation case of Equation 13, where an analogous Monte Carlo simulation was devised. These results are depicted in Figure 6. Once again, differences are on the order of 3%. Here, the two-point Gauss quadrature integration had to be modified in order to accurately calculate the integral in Equation 13 to a sufficient degree of accuracy, as discussed in Appendix A.

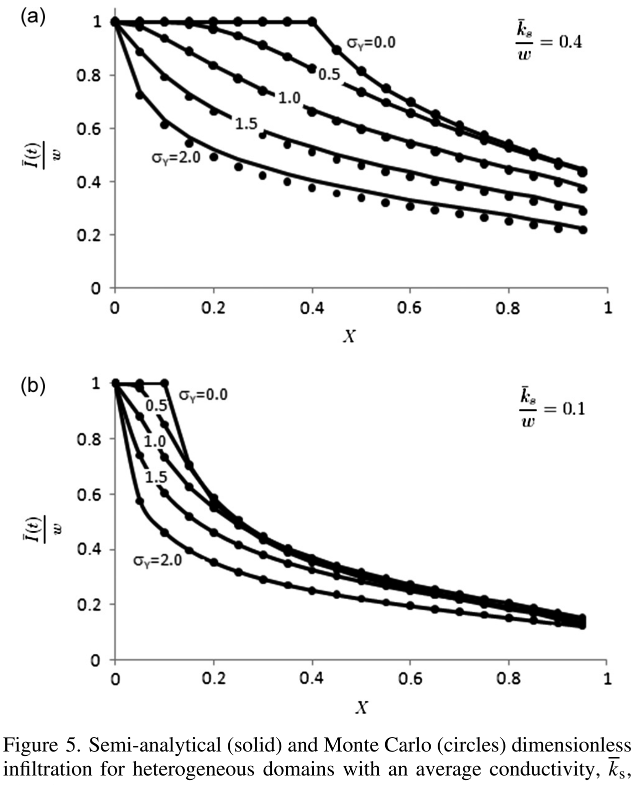

Figure 5. Semi-analytical (solid) and Monte Carlo (circles) dimensionless infiltration for heterogeneous domains with an average conductivity, $\overline{k}_s$, of 1·6 cm/h (a) and 0·4 cm/h (b), and rainfall rate of 4 cm/h. Variability in conductivity is quantified using the normalized standard deviation of log-conductivity, σ_Y, which is here varied from 0 (homogeneous) to 2 (highly heterogeneous)

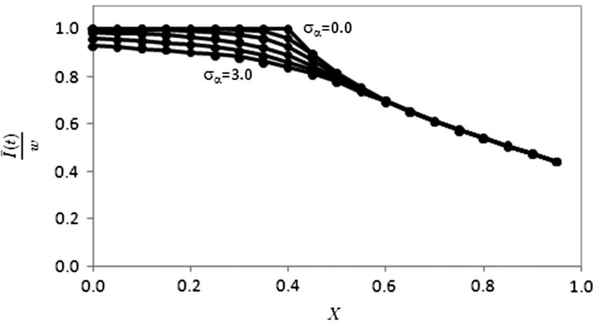

Figure 6. Analytical (solid) and Monte Carlo (circles) dimensionless infiltration curves for a homogeneous domain with spatially variable initial conditions. Here, $k_s = 1{\cdot}4$ cm/h and $w = 4$ cm/h

DISCUSSION

As it is apparent from the results, the impact of spatial variability of α and, primarily, k_s on infiltration is both calculable and significantly influences rainfall excess generation. The implications of this heterogeneity have been addressed, in part, by previous authors. We focus here primarily on the implications upon the calibration of existing homogeneous models.

As can be seen by comparing Figures 5 and 6, heterogeneity in k_s has an effect upon the asymptotic solution as time approaches infinity, while variation in α is short-lived, only directly influencing the solution, prior to and shortly after the effective (mean) ponding time. This is an indicator; heterogeneity in soil type is of much greater importance than heterogeneity in initial conditions. In addition, this indicates that variation in initial conditions will be of greater importance for short duration storms or during dry antecedent conditions. For practical purposes, it probably makes more sense to characterize the conductivity heterogeneity than the heterogeneity in initial conditions. While the two have clearly different effects, it is likely that our ability to uniquely estimate both σ_k and σ_α from field data, where this signature is filtered through additional hydrologic processes and data error, is small to non-existent.

Noteworthy is the distinct behaviour of the upscaled solution as compared to the original point-scale solution, depicted in Figure 3. It is clear that, when estimated from automatic or manual calibration to appropriate field data, the calculated hydraulic conductivity will not correspond to the average conductivity in the domain, but rather underestimates the conductivity by a factor proportional to the degree of spatial variability (see also Figures 5 and 6). This underestimation is required in order to obtain the same total infiltration volume, i.e. with a high degree of heterogeneity, the upscaled solution generates more surface runoff and less infiltration than the 'equivalent' point-scale solution. This may be the primary reason why the literature recommends an effective GA conductivity

DOI: 10.1002/hyp

value smaller than estimated from soil data (Risse *et al.* (1994); Nearing *et al.* (1996)): increased heterogeneity leads to a smaller amount of water infiltrating for a given average k_s. Strictly speaking, however, this estimate of conductivity cannot truly be considered an 'effective' value, as the transient behaviour of the upscaled (more physically realistic) solution cannot be replicated by simply using an artificially small conductivity (see also Corradini *et al.* (2002)).

CONCLUSIONS

Explicit approximations of the upscaled Green and Ampt infiltration equation have been derived, which separately consider lateral heterogeneity in saturated hydraulic conductivity (Equation 9), and wetting front matric potential, porosity, and/or initial soil moisture (Equation 13). The approximations, which neglect effects of run on or spatial correlation, have been evaluated against Monte Carlo simulations and produce results accurate to 3% of the computationally intensive 'exact' cases, at a computational cost similar to the original GA formula without upscaling. The integrals obtained from the upscaling process may be evaluated analytically or with single-interval low-order quadrature, and are therefore quite suitable for inclusion in land surface schemes and other surface water models where computational speed is a significant issue. A critical result here is that the upscaled form of the GA equation is different than the point-scale solution with upscaled parameters, indicating that calibration alone is insufficient to correctly replicate the infiltration process in heterogeneous media. 'Effective' conductivities at the basin scale that would allow direct application of the point-scale GA model to even mildly heterogeneous domains do not exist. However, approximate effective conductivities (which can match the time-integrated ratio of runoff to infiltration) will always be smaller than field-measured conductivities, with the difference proportional to the degree of soil heterogeneity.

REFERENCES

Abbott MB, Bathurst JC, Cunge JA, O'Connell P, Rasmussen J. 1986. An introduction to the european system: Systeme Hydrologique Europeen (SHE). *Journal of Hydrology* **87**: 61–77.

Barry D, Parlange J-Y, Li L, Jenge D-S, Crapper M. 2005. Green-Ampt approximations. *Advances in Water Resources* **28**: 10 1003–1009.

Bicknell BR, Imhoff JC, Kittle JL, Donigian AS, Johanson RC Jr. 2001. *Hydrological Simulation Program—FORTRAN user's manual for release 12*. U.S. EPA Ecosystem Research Division, Athens, Georgia/U.S. Geological Survey, Office of Surface Water: Reston, Virginia.

Chen Z-Q, Govindaraju RS, Kavvas ML. 1994. Spatial averaging of unsaturated flow equations under infiltration conditions over areally heterogeneous fields, 1. Development of models. *Water Resources Research* **30**: 523–533.

Chow VT, Maidment DR, Mays LW. 1988. *Applied Hydrology*. McGraw-Hill: New York.

Corradini C, Govindaraju RS, Morbidelli R. 2002. Simplified modelling of areal average infiltration at the hillslope scale. *Hydrological Processes* **16**(9): 1757–1770.

Dagan G, Bresler E. 1983. Unsaturated flow in spatially variable fields, 1. Derivation of models of infiltration and redistribution. *Water Resources Research* **19**: 413–420.

DeRoo APJ, Hazelhoff L, Heuvelink GMB. 1992. Estimating the effects of spatial variability of infiltration on the output of a distributed runoff and soil erosion model using Monte Carlo methods. *Hydrological Processes* **6**: 127–143.

Det Norske Veritas. 1997. *Statistical Representation of Soil Data*, Recommended Practice Report DNV-RP-C207, Det Norske Veritas.

Dingman SL. 2002. *Physical Hydrology*, 2nd edn, Prentice Hall: New Jersey.

Famiglietti JS, Ryu D, Berg AA, Rodell M, Jackson TJ. 2008. Field observations of soil moisture variability across scales. *Water Resources Research* **44**: w01423. DOI:10·1029/2006WR005804.

Flanagan DC, Nearing MA. 1995. *USDA-Water Erosion Prediction project: Hillslope profile and watershed model documentation*. NSERL Report No. 10. USDA-ARS National Soil Erosion Research Laboratory, West Lafayette, Ind.

Govindaraju RS, Morbidelli R, Corradini C. 2001. Areal infiltration modeling over soil with spatially-correlated hydraulic conductivities. *Journal of Hydrological Engineering* **6**: 150–158.

Green WH, Ampt G. 1911. Studies on soil physics, 1. The flow of air and water through soils. *The Journal of Agricultural Science* **4**: 1–24.

Haskett JD, Pachepsky YA, Acocka B. 1995. Use of the beta distribution for parameterizing variability of soil properties at the regional level for crop yield estimation. *Agricultural Systems* **48**: 73–86.

Lakhankar T, Ghedira H, Temimi M, Azar AE, Khanbilvardi R. 2009. Effect of land cover heterogeneity on soil moisture retrieval using active microwave remote sensing data. *Remote Sensing of Environment* **1**: 80–91.

Maller RA, Sharma ML. 1981. An analysis of areal infiltration considering spatial variability. *Journal of Hydrology* **52**: 25–37.

Mein RG, Larson CL. 1973. Modeling infiltration during a steady rain. *Water Resources Research* **9**(2): 384–394.

Merzougui M, Gifford GF. 1987. Spatial variability of infiltration rates on a semiarid seeded rangeland. *Hydrological Sciences Journal* **32**(3): 243–250.

Miller GR, Baldocchi DD, Law BE, Meyersd T. 2007. An analysis of soil moisture dynamics using multi-year data from a network of micrometeorological observation sites. *Advances in Water Resources* **30**(5): 1065–1081.

Morbidelli R, Corradini C, Govindaraju RS. 2006. A field-scale infiltration model accounting for spatial heterogeneity of rainfall and soil saturated hydraulic conductivity. *Hydrological Processes* **20**(7): 1465–1481.

Nearing MA, Liu BY, Risse LM, Zhang X. 1996. Curve numbers and Green-Ampt effective hydraulic conductivities. *Water Resources Bulletin* **32**(1): 125–136.

Neitsch SL, Arnold JG, Kiniry JR, Williams JR. 2002. *Soil Water Assessment Tool Theoretical Documentation*. Grassland, Soil and Water Research Laboratory, Agricultural Research Service: Temple, Texas.

Neuman S. 1976. Wetting front pressure head in the infiltration model of Green and Ampt. *Water Resources Research* **12**: 564–566.

Patgiri DK, Baruah TC. 1995. Spatial variability of total porosity, air entry potential and saturation water content in a cultivated inceptisol. I. Semivariance analysis. *Agricultural Water Management* **27**(1): 1–9.

Philip JR. 1957. The theory of infiltration: 4. Sorptivity and algebraic infiltration equations. *Soil Science* **84**: 257–264.

Risse LM, Nearing MA, Savabi MR. 1994. Determining the Green-Ampt effective hydraulic conductivity from rainfall-runoff data for the WEPP model. *Transactions of the ASAE* **37**(2): 411–418.

Sharma ML, Gander GA, Hunt C. 1980. Spatial variability of infiltration in a watershed. *Journal of Hydrology* **45**(1-2): 101–122.

Sivapalan M, Wood EF. 1986. Spatial heterogneity and scale in the infiltration response of catchments. *Scale Problems in Hydrology*, Reidel D (ed). Water Science and Technology Library: Dordrecht; 81–106.

Smith RE, Goodrich DC. 2000. Model for rainfall excess patterns on randomly heterogeneous area. *Journal of Hydrological Engineering* **5**: 355–362.

Verseghy DL. 1991. CLASS-A canadian land surface scheme for GCMS: I. Soil model. *International Journal of Climatology* **11**(2): 111–133.

APPENDIX

EVALUATION OF THE VARIABLY SATURATED ε INTEGRAL

The most computationally efficient and reasonably accurate means of calculating the integral in Equation 13 was found to be a combination of two-point Gauss quadrature (for earlier times, where the impacts of scaling are dominant) and the non-upscaled Lambert approximation (for later times, where upscaling has little or no effect but two-point quadrature can lead to numerical instabilities). Defining X_c as the critical X for the combination, the modified two-point Gauss quadratic integration was defined as:

$$f(t) = \begin{cases} f_{2p} & \text{for } X \leq X_c \\ f_{\text{Lambert}} & \text{for } X > X_c \end{cases}$$

where f_{2p} is the solution for single-interval two-point Gauss quadrature, f_{Lambert} is the solution of the Lambert approximation, and X_c is defined as:

$$X_c = \begin{cases} 0{\cdot}45 & \text{for } \sigma_\alpha \leq \frac{1}{3}\mu_\alpha \\ 0{\cdot}60 & \text{for } \sigma_\alpha > \frac{1}{3}\mu_\alpha \end{cases}$$

DOI: 10.1002/hyp